

# Quantification of Metabolic Products from Microbial Hosts in Complex Media Using Optically Diffracting Hydrogels

Sukwon Jung, Kelsey I. MacConaghy, Michael T. Guarnieri, Joel L. Kaar,\* and Mark P. Stoykovich\*



Cite This: <https://doi.org/10.1021/acsabm.1c01267>



Read Online

ACCESS |



Metrics & More



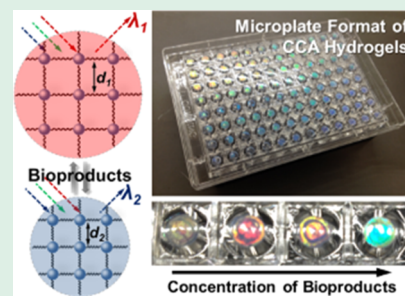
Article Recommendations



Supporting Information

**ABSTRACT:** We herein describe a highly versatile platform approach for the in situ and real-time screening of microbial biocatalysts for enhanced production of bioproducts using photonic crystal hydrogels. This approach was demonstrated by preparing optically diffracting films based on polymerized *N*-isopropylacrylamide that contracted in the presence of alcohols and organic acids. The hydrogel films were prepared in a microwell plate format, which allows for high-throughput screening, and characterized optically using a microwell plate reader. While demonstrating the ability to detect a broad range of relevant alcohols and organic acids, we showed that the response of the films correlated strongly with the octanol–water partition coefficient ( $\log P$ ) of the analyte. Differences in the secretion of ethanol and succinic acid from strains of *Zymomonas mobilis* and *Actinobacillus succinogenes*, respectively, were further detected via optical characterization of the films. These differences, which in some cases were as low as  $\sim 3$  g/L, were confirmed by high-performance liquid chromatography, thereby demonstrating the sensitivity of this approach. Our findings highlight the potential utility of this multiplexed approach for the detection of small organic analytes in complex biological media, which overcomes a major challenge in conventional optical sensing methods.

**KEYWORDS:** crystalline colloidal array, photonic crystal, metabolic engineering, synthetic biology, genome engineering, ethanol, organic acids



enhanced by eliminating the need to remove background molecules and/or replace the sensing solution prior to measurement (i.e., via extensive washing). By enabling the quantification of metabolic products in situ, such methods may enable throughputs that match the scale of diversity that can be generated by advances in metabolic and genome engineering.

## INTRODUCTION

Optically diffracting materials that are also chemically responsive offer considerable opportunities for developing biosensing technologies with broad practical implications.<sup>1–4</sup> Such technologies may be realized through embedding a crystalline colloidal array (CCA) (e.g., that consists of charged particles) within a hydrogel that swells or shrinks in the presence of a specific analyte.<sup>5–8</sup> In this arrangement, the CCA acts as a photonic crystal that produces an optical readout based on the diffraction of light. Although the field of photonic crystal hydrogels for sensing is relatively mature, the use of such materials for sensing in biological applications remains limited. Of particular interest is exploiting the advantages of photonic crystal hydrogels for sensing in complex environments such as cell culture and/or microbial growth media. Such environments present inherent challenges due to the presence of biomacromolecules, inorganic salts, sugars (e.g., glucose), and amino acids, which can interfere with optical detection.

A particularly intriguing area where photonic crystal hydrogels may have ample utility for sensing is in the fields of metabolic and genome engineering. In these fields, the need for robust screening tools that can quantify the biological conversion of renewable substrates to excreted products (e.g., fuels or chemicals) in a complex biological milieu is critical.<sup>9,10</sup> Importantly, the throughput of such tools may be markedly

enhanced by eliminating the need to remove background molecules and/or replace the sensing solution prior to measurement (i.e., via extensive washing). By enabling the quantification of metabolic products in situ, such methods may enable throughputs that match the scale of diversity that can be generated by advances in metabolic and genome engineering. Owing to the throughput necessary to screen large libraries of genomic mutations, eliminating the need for exogenous reagents (e.g., enzymes, co-factors, and fluorophores) would also be beneficial.<sup>11</sup> Such tools would further ideally be compatible with screening a broad range of small molecules (e.g., alcohols, organic acids, lipids, etc.) with high sensitivity using routine instrumentation. To date, a universal screening platform that meets these requirements remains elusive, thereby restricting the ability to efficiently analyze large libraries to capture beneficial mutations. Notably, conventional methods for screening large libraries for metabolic and genome engineering include high-performance liquid chromatography

**Received:** December 16, 2021

**Accepted:** February 1, 2022

(HPLC), liquid or gas chromatography, tandem mass spectrometry, and flow cytometry.<sup>12–17</sup>

In this work, we sought to investigate the utility of photonic crystal hydrogels for metabolic and genome engineering applications, including the detection of alcohols and organic acids in microbial culture media. Alcohol- and acid-responsive photonic crystal hydrogels were prepared via photopolymerization of poly(*N*-isopropylacrylamide) (pNIPAM)-based films. The films, which contained negatively charged polystyrene (PS) particles, were polymerized in the wells of 96-well microplates to allow for optical characterization using a UV/vis microplate reader. Following polymerization, the responsive nature of the films to various alcohols and organic acids was characterized as a function of solvent properties. The detection of ethanol and succinic acid in culture media was further demonstrated using *Zymomonas mobilis* and *Actinobacillus succinogenes* strains as model host organisms.<sup>18–21</sup> While used as model analytes in this work, ethanol and succinic acid are of relevance as biofuels and platform chemicals for producing plastics, textiles, pharmaceutical compounds, organic solvents, and food additives. Quantitative HPLC was further used to correlate the production of ethanol and succinic acid from each model strain with the film response.

## MATERIALS AND METHODS

**Materials.** *N*-Isopropylacrylamide (NIPAM) was purchased from Sigma-Aldrich (St. Louis, MO) and purified by solubilization in hexane at 60 °C followed by precipitation in an ice bath. The resulting precipitate was filtered and stored at 4 °C for further use. Styrene and divinylbenzene were purchased from Sigma-Aldrich and purified via chromatography using an aluminum oxide-packed column prior to use. Analytical-grade *N,N'*-methylenebis(acrylamide) (MBAA), *N*-hydroxyethyl acrylamide (HEAA), 3-(trimethoxysilyl)propyl methacrylate, 2-hydroxy-4'-(2-hydroxyethoxy)-2-methylpropiophenone (water-soluble photoinitiator, Irgacure 2959), ammonium persulfate, target chemicals (i.e., methanol, ethanol, 1-propanol, 2-propanol, 1,3-propanediol, 1-butanol, 1,4-butanediol, acetic acid, propionic acid, lactic acid, 3-hydroxypropionic acid, butyric acid, succinic acid, and adipic acid), sodium 1-allyloxy-2-hydroxypropane sulfonate (COPS-1) ionic comonomer, and Aerosol MA-80-1 surfactant were purchased from Sigma-Aldrich and used without further purification. Aluminum oxide anhydrous powder and sodium bicarbonate were purchased from Fisher Scientific (Waltham, MA) and used as received. Additionally, biotechnology-grade ion-exchange mixed bed resin (AG 501-X8) and 96-well plates with UV-transparent well bottoms were obtained from Bio-Rad (Hercules, CA) and Corning Inc. (Corning, NY), respectively. Furthermore, the PS nanospheres were prepared by emulsion polymerization and characterized by dynamic light scattering to determine particle size and monodispersity.<sup>5</sup> The PS nanospheres had a diameter and polydispersity of ~110 nm and 3.4%, respectively. Figure S1 shows a representative scanning electron microscopy image of the free nanospheres prior to incorporation into the hydrogel films.

**Fabrication of Photonic Crystal Hydrogels.** Photonic crystal hydrogels were fabricated in the microwells of 96-well plates by initially functionalizing the surface of the wells with methacrylate groups. Surface functionalization was enabled by initially treating the plates with UV/ozone (Novascan UV Ozone Cleaner, Ames, IA) for 15 min and subsequently adding 3% (v/v) 3-(trimethoxysilyl)propyl methacrylate in cyclohexane to each well for 2 h. Each well was rinsed with ethanol, and the plate was dried at 40 °C for 1 h. The plate was then covered with aluminum foil and stored at room temperature prior to use. At the time of use, a pre-gel solution consisting of 975 mM NIPAM, 25 mM HEAA, 10 mM MBAA, 0.05% (w/v) Irgacure 2959, 7% (w/v) charged PS nanospheres, and 15% (v/v) DMSO was added to each well. To ensure CCA formation, the pre-gel solution was mixed with the ion-exchange resin and incubated at room

temperature in the dark for 1 h and spun down via centrifugation prior to use. To create uniform films in the wells, an acrylic mold with pins was pushed into the wells, after which the wells were illuminated with 312 nm UV light with an 8 W handheld UV lamp (Spectronics Corp., Westbury, NY) for 90 min at 4 °C. Notably, the slow polymerization rate at a low temperature allowed the CCA to retain its photonic crystal structure during polymerization. Upon removal of the mold, the CCA hydrogel films, which had an approximate thickness of ~175 μm, were subsequently rinsed and stored with ultrapure water prior to use.

**Optical Characterization.** Optical diffraction of the hydrogels in a microplate format was characterized quantitatively using an Infinite 200 PRO microspectrophotometer (Tecan Systems Inc., San Jose, CA). For quantitative characterization, the 96-well plate was incubated with microbial culture samples or aqueous solutions containing alcohols or acids at high ionic strength (250 mM NaCl) for 30 min at the desired temperature (26 or 28 °C). The wavelength of peak diffraction was specifically determined by measuring the attenuation of the hydrogel films between 350 and 850 nm while using a step size of 2 nm.

**Growth of *Z. mobilis* and *A. succinogenes*.** *Z. mobilis* was cultivated and grown in minimal media containing K<sub>2</sub>HPO<sub>4</sub>, 1 g/L; KH<sub>2</sub>PO<sub>4</sub>, 1 g/L; NaCl, 0.5 g/L; (NH<sub>4</sub>)<sub>2</sub>SO<sub>4</sub>, 1 g/L; MgSO<sub>4</sub>·7H<sub>2</sub>O, 0.2 g/L; CaCl<sub>2</sub>·2H<sub>2</sub>O, 0.2 g/L; Na<sub>2</sub>MoO<sub>4</sub>·2H<sub>2</sub>O, 0.025 g/L; FeSO<sub>4</sub>·7H<sub>2</sub>O, 0.025 g/L; Ca-pantothenate, 5 mg/L; pyridoxine, 1 mg/L; biotin, 1 mg/L; nicotinic acid, 1 mg/L; and glucose, 20 g/L. *Z. mobilis* was outgrown overnight from cell stocks stored at –70 °C in 10 mL of pre-seed medium in a 15 mL conical tube. Seed cultures were inoculated at optical density (OD 600 nm) = 0.1 into sealed 150 mL shake flasks equipped with twin bubble airlocks to initiate fermentation at 33 °C with 100 rpm shaking. Following 48 h of cultivation, cultures were harvested via centrifugation, and culture supernatants were vacuum-filtered using 0.2 μm Steriflip filter units (MilliporeSigma, USA). *A. succinogenes* 130Z (ATCC 55618) was cultivated anaerobically in 50 ml of mock hydrolysate (Fluka Analytical, India) at 37 °C and 120 rpm. Serum bottle cultures were inoculated at an optical density at 600 nm of ~0.1 with plate-harvested biomass. Following 48 h of cultivation, culture supernatants were isolated as described above for *Z. mobilis*.

**HPLC Analysis.** The concentration of ethanol and succinic acid in samples was analyzed using a Shimadzu (Kyoto, Japan) 10avp HPLC instrument equipped with an Aminex HPX-87H column (Bio-rad, Hercules, CA). Prior to HPLC analysis, the media samples were filtered using centrifugal filtration devices with 0.22 μm pores (Costar Spin-X, Corning, NY). For analysis, 40 μL samples were injected in the pre-heated column (50 °C) with the mobile phase (5 mM sulfuric acid) at a flow rate of 0.6 mL/min. For quantitative analysis, calibration curves for ethanol and succinic acids were constructed using standard samples. Specifically, aqueous solutions with known concentrations of ethanol (0–120 g/L) and succinic acids (0–30 g/L) were injected into the column, and characteristic peak areas of each chemical were computed. The concentration of each analyte was then plotted with the corresponding peak area.

## RESULTS AND DISCUSSION

**Fabrication and Optical Characterization of Responsive Hydrogels in 96-Well Microplates.** Films for optical detection were prepared in the wells of 96-well microplates with a uniform thickness of ~175 μm as we described previously.<sup>22</sup> As shown in Figure 1A, the mold was inserted into the wells after addition of a pre-gel solution, which contained pNIPAM, HEAA, MBAA, Irgacure 2959, and sulfonated PS particles (7% (w/v); 110 nm diameter). After insertion of the mold, the microplate was illuminated with 312 nm light, resulting in the formation of a cross-linked network. Methacrylate groups on the surface of the wells and PS particles allowed bonding of the network to the plate and covalent incorporation of the PS particles in the resulting film.

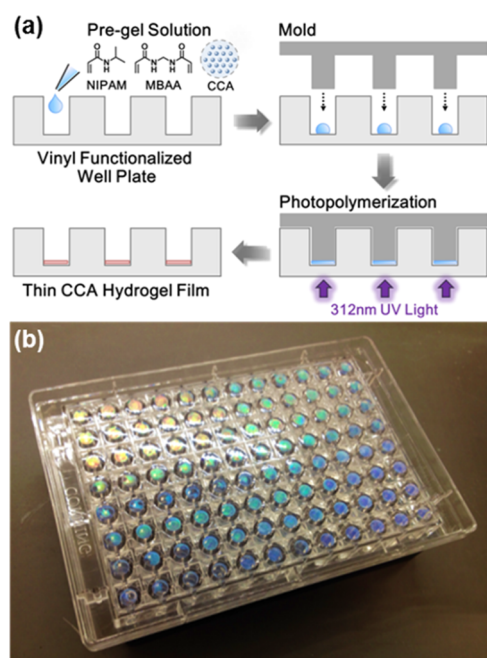


**Figure 1.** Preparation of 96-well plates of optically diffracting pNIPAM-based films containing negatively charged PS particles that are self-assembled into a CCA. (a) Schematic of the fabrication process, which involves the use of an acrylic mold to ensure uniformity of the films. (b) Photograph of a representative microplate showing the effect of temperature on the coloration of the optically diffracting films in each well.

Particles of the specified size were used to enable optical characterization of the films in the visible range. It is well understood that varying the particle size can change the lattice spacing and thus the wavelength of peak diffraction.<sup>23</sup>

By enabling the use of a UV/vis microplate reader to measure optical diffraction, fabrication of the films in 96-well microplates permits multiplexed, high-throughput characterization. We have previously demonstrated that the wavelength of peak diffraction for such films exhibits a characteristic blue shift in the presence of organic analytes, including ethanol.<sup>22</sup> This blue shift is the result of the contraction of the films due to the change in the solvent quality and thus in the polymer–solution Flory–Huggins interaction parameter ( $\chi$ ) upon addition of the analyte (see Figure S2 for representative raw attenuation spectra of the hydrogel films as a function of ethanol concentration). Contraction of the film in turn leads to a decrease in the lattice spacing of the PS particles, which underlies the optical response as explained by the Bragg–Snell law.<sup>24–26</sup> The addition of an organic analyte specifically results in a concentration-dependent increase in  $\chi$  for the polymer–solution interactions. Given that  $\chi$  is also a function of temperature, the impact of changes to  $\chi$  on the optical response of the films could be observed by varying the temperature across the microplate. Figure 1B clearly shows the change in coloration of the films in a representative microplate as a function of temperature, ranging from orange-yellow at the top left corner to violet at the bottom right. The gradient in color from orange-yellow to violet is indicative of increasing temperature and denotes greater contraction of the films.

Importantly, the sensitivity of photonic crystal hydrogels consisting of stimuli-responsive polymers such as pNIPAM may be rationally tuned for the detection of small molecule

analytes. By modulating the lower critical solution temperature of such hydrogels relative to the characterization temperature, we have previously demonstrated that it is possible, in effect, to maximize the extent of the response to target analytes.<sup>22</sup> Using ethanol as a model analyte, we demonstrated that photonic crystal detectors may be optimized for greater optical sensitivity by controlling the composition of the hydrogels, the temperature at which characterization is performed, and the ionic strength of the solution. In the current work, this understanding was leveraged to enhance the sensitivity of the hydrogel films, including the use of high ionic strength of the solution for characterization. By using high ionic strength, electrostatic interactions between the analyte and the film may be shielded, thereby limiting their impact on polymer–solvent interactions.

**Sensitivity of Optically Diffracting Hydrogels to Alcohols and Organic Acids.** Having demonstrated the responsive nature of the pNIPAM-based films, the sensitivity of the photonic crystal films to a library of structurally diverse short-chain alcohols and organic acids was characterized. By examining structurally diverse alcohols and acids (measured at concentrations of 64 g/L for alcohols or 15 g/L for acids), the impact of the molecular features of the analytes on the responsiveness of the films was determined. The library of molecules examined specifically included linear primary and secondary alcohols and acids, as well as diols and diacids, which represent common target molecules for synthetic biology.<sup>27–33</sup> Many of the alcohols characterized here have potential utility as renewable fuels, while the acids are potential platform chemicals for biobased polymers and secondary chemicals for diverse industries. Interestingly, the sensitivity of the optical response could be correlated to the hydrophobicity of the alcohols and acids. This was evident in Figure 2 where the optical response for some alcohols and acids (e.g., 1,3-propanediol and 1,4-butanediol) was negligible, while the response for others (e.g., 1-propanol, 1-butanol, butyric acid, and adipic acid) corresponded to the maximum attainable blue shift ( $\sim 200$  nm). The maximum blue shift occurred when the wavelength of peak diffraction shifted outside the measurable range due to contraction of the films.

**Correlation of Analyte Properties and Optical Response.** As shown in Figure 2, there was a particularly close correlation between the optical response of the photonic crystal films and the octanol–water partition coefficient ( $\log P$ ) of the organic analytes. Specifically, analytes with a larger  $\log P$ , which is indicative of increased hydrophobicity, tended to elicit a larger response, while analytes with a lower  $\log P$  elicited smaller responses. This may be explained in terms of the replacement of favorable water–polymer interactions with less favorable analyte–polymer interactions. When favorable water–polymer interactions are replaced with less favorable analyte–polymer interactions (as is the case for molecules with a large  $\log P$ ), the value of  $\chi$  of the system will increase, leading to contraction of the film and ultimately a blue shift in the wavelength of peak diffraction. Additionally, for a given  $\log P$ , it was notable that the sensitivity of the response was generally larger for the organic acids (orange shaded region) than the alcohols (blue shaded region). This was particularly notable since the concentration of the organic acids used for optical characterization (15 g/L) was considerably lower than that used for the alcohols (64 g/L), and since such photonic crystal films generally have higher sensitivities at higher analyte concentrations due to their nonlinear response to concen-

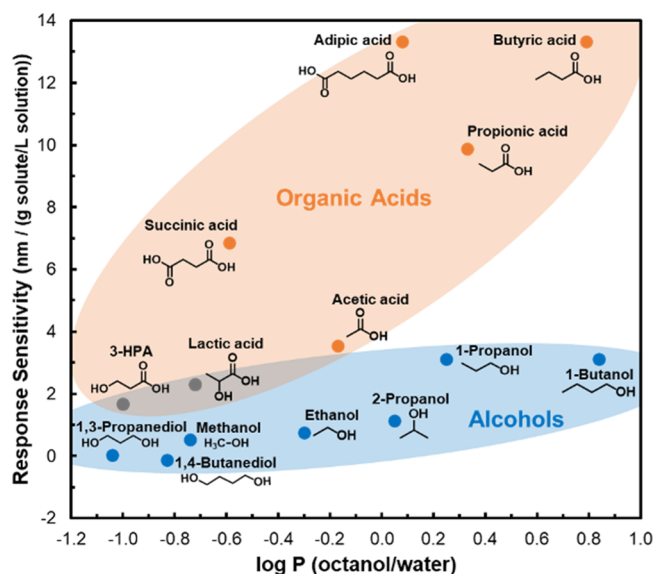


**Figure 2.** Sensitivity of the detector response as a function of the octanol–water partition coefficient parameter  $\log P$  for a library of small molecule alcohol (highlighted in blue) and organic acid (in orange) analytes. The response sensitivity is reported as the blue shift in peak diffraction wavelength (in nm) per concentration of solute (in g/L). The alcohols and organic acids were added at 64 and 15 g/L, respectively, and incubated with the films at 28 °C for 30 min prior to the measurements. Each data point represents the average measured from 6 distinct microwells per analyte, and the standard deviation of the trials while not shown as error bars, was less than 0.2 nm/(g/L).

tration. This finding suggests that the interaction of hydroxyl groups with the polymer was more favorable than the interaction of carboxylic acid groups with the polymer (as was observed for propionic acid relative to 1-propanol, which have approximately the same  $\log P$ ). Importantly, as noted above, the high ionic strength of the measurement solution would effectively screen any electrostatic interactions between the organic acids and the films. Given this, it is highly unlikely that the higher sensitivity of the films to the organic acids was due to the deprotonation of the acid groups at the measurement pH.

Further analysis of the optical response of the photonic crystal films to the analytes revealed interesting trends within the alcohol and acid groups. For example, as can be seen in Figure 2, the sensitivity of the films to primary alcohols generally increased with the number of hydrophobic methyl groups. This trend is further shown in Figure S3, which summarizes the responses for C2–C5 primary alcohols at varying analyte concentrations. Notably, the blue shift in the wavelength of peak diffraction for 1-pentanol at a concentration of 4 g/L (>200 nm) was significantly larger than that for 1-butanol at a concentration of 8 g/L (~50 nm). A similar trend in terms of the number of hydrophobic methyl groups was observed for the organic acids, although the effect of concentration on the response was not explored. Additionally, it was interesting that diols 1,3-propanediol and 1,4-butanediol elicited a smaller response than their primary alcohol counterparts (i.e., 1-propanol and 1-butanol). In addition to having a lower  $\log P$ , this is likely because the hydrophobic methyl groups in the diols are in between the hydroxyl groups and thus shielded from interacting with the polymer. Conversely, the diacids elicited a larger response than the monofunctionalized acids, which is consistent with the

interaction of carboxylic acids with the polymer being unfavorable. Interestingly, 3-hydroxypropionic acid and lactic acid, which have both carboxylic acid and alcohol groups, elicit responses that are in between that of the corresponding diol and diacid with similar chain lengths. Finally, it was also interesting that the secondary alcohol 2-propanol elicited a smaller response than 1-propanol, given they have an identical number of carbon atoms. This may be attributed to shielding of the carbons by the hydroxyl group in 2-propanol, which reduces the extent to which these groups may interact with the polymer compared to that in 1-propanol.

**In Situ Detection of Ethanol and Succinic Acid.** To demonstrate the in situ detection of ethanol produced by *Z. mobilis*, spent growth media from wild-type (WT) and five mutated variants (S1–S5) of *Z. mobilis* was added to separate wells in a test microplate. The spent media in which glucose was fully consumed consisted of supernatant from individual cultures of the WT and variants after spinning down the cells. Following incubation of the spent media in the wells at 26 °C for 30 min, the wavelength of peak diffraction was measured. Blue shifts were then computed using the diffraction wavelength elicited by the WT sample as a reference. Interestingly, while media from variants S1–S4 elicited a red-shifted response relative to WT *Z. mobilis*, the blue shift from variant S5 was markedly larger than of WT *Z. mobilis* (Figure 3A). Given that the secretion of bioproducts other than ethanol by *Z. mobilis* has been shown to be low,<sup>34</sup> this suggests that variant S5 produced significantly more ethanol than its WT counterpart. The difference in the diffraction induced by the samples can further be seen visually in the inset images in Figure 3A. To confirm the differences in ethanol production, namely between variant S5 and WT *Z. mobilis*, the concentration of ethanol in the media samples was quantified by HPLC (Figure S4 and Table S1). Notably, the results of HPLC indicated that the concentration of ethanol in the media from sample S5 was 94.8 g/L compared to 76.5 g/L from WT *Z. mobilis*. In further agreement with the above results, the concentration of ethanol from WT *Z. mobilis* was in fact greater than the concentration of ethanol from samples S1–S4. The correlation between the extent of blue shift and the concentration of ethanol in the samples is shown in Figure 3B. As we have shown in prior work for pNIPAM-based films,<sup>22</sup> this correlation was nonlinear, with the sensitivity of the films to ethanol increasing with increasing ethanol concentration. These results demonstrate the utility of this approach as a platform screening tool for in situ screening, which could easily be extended to a 384 or even 1536-well microplate format.

Succinic acid production from *A. succinogenes* was characterized in an analogous experiment by quantifying the extent of blue shift once again from the growth media. Unlike in the experiment with *Z. mobilis*, where samples were only analyzed upon full consumption of glucose, samples, in this case, were removed and analyzed periodically during growth (at 7 and 47 h). As such, the supernatant of the samples contained various carbon sources, including glucose, xylose, galactose, and arabinose, in addition to the succinic acid that was secreted by *A. succinogenes*. Additionally, because the optically diffracting films were fully contracted by the end of the growth period (using the same incubation conditions and measurement temperature as for the samples from *Z. mobilis*), the samples were diluted twofold with deionized water prior to incubation with the films. The results of optical characterization of the films showed a clear increase in the extent of blue

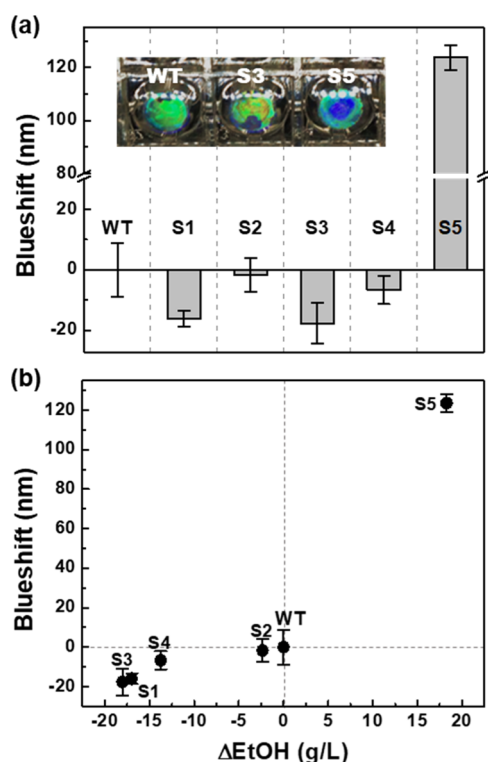


**Figure 3.** Screening of WT and mutated variants of *Z. mobilis* using the photonic crystal films in microplate format. (a) Blue shifts for the variants of *Z. mobilis* relative to the WT response to ethanol present in the spent growth media. Insets show representative photos of microwells upon incubation with samples from WT, S3, and S5 strains. (b) Correlation between the blue shift in optical response and ethanol production relative to WT *Z. mobilis* by HPLC. Error bars represent one standard deviation as measured from six independent microwells per sample. The response of the films to ethanol was measured at 26 °C since the films were fully contracted in the presence of the depleted media at 28 °C (the temperature used earlier to characterize the sensitivity of the films to alcohols and acids).

shift from both WT and mutated *A. succinogenes* samples over time (Figure 4). The exponential increase in the extent of blue shift was indicative of the increase in production and thus accumulation of succinic acid over time in the growth media. Such an increase is consistent with the expected growth rate of *A. succinogenes* during the exponential growth phase. Crucial to

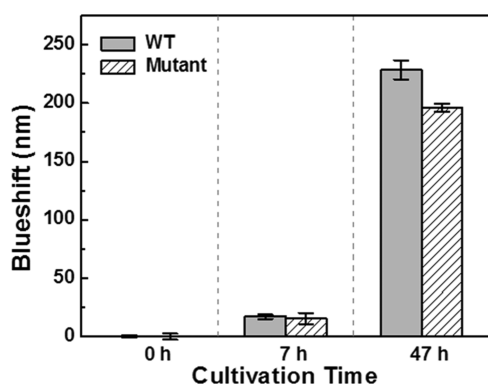


**Figure 4.** Response of the photonic crystal microplate to the media diluted twofold from WT (solid gray) and mutant (striped) strains of *A. succinogenes* during growth. Error bars represent one standard deviation as measured from six independent microwells per sample.

the success of this approach, our findings demonstrate that the expected red shift from the consumption of carbon sources in the media was smaller than the blue shift from the accumulation of succinic acid (Table S2). While crucial, this was not surprising given that glucose (and the other sugars) is significantly less hydrophobic than succinic acid (glucose has a log *P* of  $-2.6$  vs  $-0.71$  for succinic acid). Furthermore, we confirmed using HPLC that the difference in blue shift (33 nm) for the WT and mutated strain of *A. succinogenes* at 47 h was significant (Table S2). Notably, the concentration of succinic acid in the sample for the WT strain at 47 h was 25.1 g/L, whereas the concentration in the sample for the mutated strain was 22.3 g/L (Table S2). Given the minimal difference in succinic acid production between the WT and mutated strain, our findings demonstrate the sensitivity of our approach and its utility for real-time screening.

## CONCLUSIONS

In summary, our results show the application of pNIPAM-based photonic crystal films for the in situ and real-time monitoring of a broad range of relevant bioproducts of current interest in synthetic biology. While demonstrating the utility of this approach, our findings also highlight its potential for high-throughput screening in the presence of complex growth media. Of particular relevance for high-throughput screening was the ability to detect small differences in succinic acid production from *A. succinogenes* despite the consumption of carbon sources during growth. This finding highlights the sensitivity of the optical response of the films to the desired analyte. Additionally, our findings elucidate the role of the hydrophobicity of the analyte, as captured by the log *P* parameter, on the sensitivity of the optical response of the films. Based on this, it is interesting to consider how the relationship between the sensitivity of the optical response and the molecular structure of a given analyte may be optimized further by tuning the film composition. Although not explored here, the interactions of the hydrogels with their solvent environment may be rationally tuned by varying the relative fraction of the hydrophilic comonomer HEAA in the films and/or by incorporating hydrophobic comonomers.<sup>35,36</sup> Such tunability and versatility ultimately have considerable implications for the translation of this approach as a universal screening platform for analyzing large genomic libraries.

## ASSOCIATED CONTENT

### Supporting Information

The Supporting Information is available free of charge at <https://pubs.acs.org/doi/10.1021/acsabm.1c01267>.

Representative scanning electron micrographs of PS nanospheres used to assemble the CCA, optical characterization of the CCA hydrogel microplate platform, blue shift of photonic crystal films to C2–C5 primary alcohols at varying analyte concentrations, HPLC traces of reference samples and media for the WT and S5 variant of *Z. mobilis*, quantification of ethanol concentration from media for the WT and S1–S5 variants from HPLC analysis, and quantification of sugar and succinic acid concentration from media for WT and mutated *A. succinogenes* as a function of growth time by HPLC analysis (PDF)

## AUTHOR INFORMATION

### Corresponding Authors

Joel L. Kaar – Department of Chemical and Biological Engineering, University of Colorado, Boulder, Colorado 80303, United States; [orcid.org/0000-0002-0794-3955](https://orcid.org/0000-0002-0794-3955); Email: [joel.kaar@colorado.edu](mailto:joel.kaar@colorado.edu)

Mark P. Stoykovich – Pritzker School of Molecular Engineering, University of Chicago, Chicago, Illinois 60637, United States; Email: [stoykovich@uchicago.edu](mailto:stoykovich@uchicago.edu)

### Authors

Sukwon Jung – Department of Chemical and Biological Engineering, University of Colorado, Boulder, Colorado 80303, United States

Kelsey I. MacConaghy – Department of Chemical and Biological Engineering, University of Colorado, Boulder, Colorado 80303, United States

Michael T. Guarnieri – Biosciences Center, National Renewable Energy Laboratory, Golden, Colorado 80401, United States

Complete contact information is available at: <https://pubs.acs.org/10.1021/acsabm.1c01267>

### Notes

The authors declare no competing financial interest.

## ACKNOWLEDGMENTS

This work was supported by funding from the National Science Foundation (DMR1411320) and the Department of Energy, Office of Energy Efficiency and Renewable Energy (DE-AC36-08GO28308). The authors also thank Héctor Sánchez-Morán for carefully reading and providing assistance with the preparation of the manuscript.

## REFERENCES

- (1) Jung, S.; Kaar, J. L.; Stoykovich, M. P. Design and Functionalization of Responsive Hydrogels for Photonic Crystal Biosensors. *Mol. Syst. Des. Eng.* **2016**, *1*, 225–241.
- (2) Wang, J.; Pinkse, P. W. H.; Segerink, L. I.; Eijkel, J. C. T. Bottom-Up Assembled Photonic Crystals for Structure-Enabled Label-Free Sensing. *ACS Nano* **2021**, *15*, 9299–9327.
- (3) Liao, J.; Ye, C.; Agrawal, P.; Gu, Z.; Zhang, Y. S. Colloidal Photonic Crystals for Biomedical Applications. *Small Struct.* **2021**, *2*, 2000110.
- (4) Shen, P.; Zhang, Y.; Cai, Z.; Liu, R.; Xu, X.; Li, R.; Wang, J.-J.; Yang, D. a. Three-Dimensional/Two-Dimensional Photonic Crystal Hydrogels for Biosensing. *J. Mater. Chem. C* **2021**, *9*, 5840–5857.
- (5) Macconaghy, K. I.; Geary, C. I.; Kaar, J. L.; Stoykovich, M. P. Photonic Crystal Kinase Biosensor. *J. Am. Chem. Soc.* **2014**, *136*, 6896–6899.
- (6) MacConaghy, K. I.; Chadly, D. M.; Stoykovich, M. P.; Kaar, J. L. Optically Diffracting Hydrogels for Screening Kinase Activity in Vitro and in Cell Lysate: Impact of Material and Solution Properties. *Anal. Chem.* **2015**, *87*, 3467–3475.
- (7) MacConaghy, K. I.; Chadly, D. M.; Stoykovich, M. P.; Kaar, J. L. Label-Free Detection of Missense Mutations and Methylation Differences in the P53 Gene Using Optically Diffracting Hydrogels. *Analyst* **2015**, *140*, 6354–6362.
- (8) Yan, Z.; Xue, M.; He, Q.; Lu, W.; Meng, Z.; Yan, D.; Qiu, L.; Zhou, L.; Yu, Y. A Non-Enzymatic Urine Glucose Sensor with 2-D Photonic Crystal Hydrogel. *Anal. Bioanal. Chem.* **2016**, *408*, 8317–8323.
- (9) Yang, J.; Kim, B.; Kim, G. Y.; Jung, G. Y.; Seo, S. W. Synthetic Biology for Evolutionary Engineering: From Perturbation of Genotype to Acquisition of Desired Phenotype. *Biotechnol. Biofuels* **2019**, *12*, 113.
- (10) Zeng, W.; Guo, L.; Xu, S.; Chen, J.; Zhou, J. High-Throughput Screening Technology in Industrial Biotechnology. *Trends Biotechnol.* **2020**, *38*, 888–906.
- (11) Correa, E.; Sletta, H.; Ellis, D. I.; Hoel, S.; Ertesvag, H.; Ellingsen, T. E.; Valla, S.; Goodacre, R. Rapid Reagentless Quantification of Alginate Biosynthesis in *Pseudomonas Fluorescens* Bacteria Mutants Using FT-IR Spectroscopy Coupled to Multivariate Partial Least Squares Regression. *Anal. Bioanal. Chem.* **2012**, *403*, 2591–2599.
- (12) Liu, R.; Liang, L.; Freed, E. F.; Choudhury, A.; Eckert, C. A.; Gill, R. T. Engineering Regulatory Networks for Complex Phenotypes in *E. Coli*. *Nat. Commun.* **2020**, *11*, 4050.
- (13) Gowers, G. O. F.; Chee, S. M.; Bell, D.; Suckling, L.; Kern, M.; Tew, D.; McClymont, D. W.; Ellis, T. Improved Betulinic Acid Biosynthesis Using Synthetic Yeast Chromosome Recombination and Semi-Automated Rapid LC-MS Screening. *Nat. Commun.* **2020**, *11*, 868.
- (14) Duarte, J. M.; Barbier, I.; Schaerli, Y. Bacterial Microcolonies in Gel Beads for High-Throughput Screening of Libraries in Synthetic Biology. *ACS Synth. Biol.* **2017**, *6*, 1988–1995.
- (15) Bowman, E. K.; Alper, H. S. Microdroplet-Assisted Screening of Biomolecule Production for Metabolic Engineering Applications. *Trends Biotechnol.* **2020**, *38*, 701–714.
- (16) Gajewski, J.; Buelens, F.; Serdjukow, S.; Janßen, M.; Cortina, N.; Grubmüller, H.; Grninger, M. Engineering Fatty Acid Synthases for Directed Polyketide Production. *Nat. Chem. Biol.* **2017**, *13*, 363–365.
- (17) Yu, Y.; Chang, P.; Yu, H.; Ren, H.; Hong, D.; Li, Z.; Wang, Y.; Song, H.; Huo, Y.; Li, C. Productive Amyrin Synthases for Efficient  $\alpha$ -Amyrin Synthesis in Engineered *Saccharomyces Cerevisiae*. *ACS Synth. Biol.* **2018**, *7*, 2391–2402.
- (18) Li, Y.; Zhai, R.; Jiang, X.; Chen, X.; Yuan, X.; Liu, Z.; Jin, M. Boosting Ethanol Productivity of *Zymomonas Mobilis* 8b in Enzymatic Hydrolysate of Dilute Acid and Ammonia Pretreated Corn Stover Through Medium Optimization, High Cell Density Fermentation and Cell Recycling. *Front. Microbiol.* **2019**, *10*, 2316.
- (19) Yang, S.; Fei, Q.; Zhang, Y.; Contreras, L. M.; Utturkar, S. M.; Brown, S. D.; Himmel, M. E.; Zhang, M. *Zymomonas Mobilis* as a Model System for Production of Biofuels and Biochemicals. *Microb. Biotechnol.* **2016**, *9*, 699–717.
- (20) Guarnieri, M. T.; Chou, Y. C.; Salvachua, D.; Mohagheghi, A.; St John, P. C.; Peterson, D. J.; Bomble, Y. J.; Beckham, G. T. Metabolic Engineering of *Actinobacillus Succinogenes* Provides Insights into Succinic Acid Biosynthesis. *Appl. Environ. Microbiol.* **2017**, *83*, No. e00996-17.
- (21) Brink, H. G.; Nicol, W. Succinic Acid Production with *Actinobacillus Succinogenes*: Rate and Yield Analysis of Chemostat and Biofilm Cultures. *Microb. Cell Factories* **2014**, *13*, 111.
- (22) Jung, S.; MacConaghy, K. I.; Kaar, J. L.; Stoykovich, M. P. Enhanced Optical Sensitivity in Thermoresponsive Photonic Crystal Hydrogels by Operating Near the Phase Transition. *ACS Appl. Mater. Interfaces* **2017**, *9*, 27927–27935.
- (23) Carlson, R. J.; Asher, S. A. Characterization of Optical Diffraction and Crystal Structure in Monodisperse Polystyrene Colloids. *Appl. Spectrosc.* **1984**, *38*, 297–304.
- (24) Asher, S. A.; Holtz, J.; Liu, L.; Wu, Z. Self-Assembly Motif for Creating Submicron Periodic Materials. Polymerized Crystalline Colloidal Arrays. *J. Am. Chem. Soc.* **1994**, *116*, 4997–4998.
- (25) Tang, W.; Chen, C. Hydrogel-Based Colloidal Photonic Crystal Devices for Glucose Sensing. *Polymers* **2020**, *12*, 625.
- (26) Zhang, H.; Bu, X.; Yip, S.; Liang, X.; Ho, J. C. Self-Assembly of Colloidal Particles for Fabrication of Structural Color Materials toward Advanced Intelligent Systems. *Adv. Intell. Syst.* **2020**, *2*, 1900085.
- (27) Liang, L.; Liu, R.; Freed, E. F.; Eckert, C. A. Synthetic Biology and Metabolic Engineering Employing *Escherichia Coli* for C2–C6 Bioalcohol Production. *Front. Bioeng. Biotechnol.* **2020**, *8*, 710.

(28) Tian, L.; Papanek, B.; Olson, D. G.; Rydzak, T.; Holwerda, E. K.; Zheng, T.; Zhou, J.; Maloney, M.; Jiang, N.; Giannone, R. J.; Hettich, R. L.; Guss, A. M.; Lynd, L. R. Simultaneous Achievement of High Ethanol Yield and Titer in *Clostridium Thermocellum*. *Biotechnol. Biofuels* **2016**, *9*, 116.

(29) Dong, H.; Zhao, C.; Zhang, T.; Zhu, H.; Lin, Z.; Tao, W.; Zhang, Y.; Li, Y. A Systematically Chromosomally Engineered *Escherichia Coli* Efficiently Produces Butanol. *Metab. Eng.* **2017**, *44*, 284–292.

(30) Horinouchi, T.; Sakai, A.; Kotani, H.; Tanabe, K.; Furusawa, C. Improvement of Isopropanol Tolerance of *Escherichia Coli* Using Adaptive Laboratory Evolution and Omics Technologies. *J. Biotechnol.* **2017**, *255*, 47–56.

(31) Liu, J.; Li, J.; Shin, H.-d.; Liu, L.; Du, G.; Chen, J. Protein and Metabolic Engineering for the Production of Organic Acids. *Bioresour. Technol.* **2017**, *239*, 412–421.

(32) Becker, J.; Lange, A.; Fabarius, J.; Wittmann, C. Top Value Platform Chemicals: Bio-Based Production of Organic Acids. *Curr. Opin. Biotechnol.* **2015**, *36*, 168–175.

(33) Li, Y.; Yang, S.; Ma, D.; Song, W.; Gao, C.; Liu, L.; Chen, X. Microbial Engineering for the Production of C2-C6 organic Acids. *Nat. Prod. Rep.* **2021**, *38*, 1518–1546.

(34) Tsantili, I. C.; Karim, M. N.; Klapa, M. I. Quantifying the Metabolic Capabilities of Engineered *Zymomonas Mobilis* Using Linear Programming Analysis. *Microb. Cell Factories* **2007**, *6*, 8.

(35) Li, S.; Davis, E. N.; Huang, X.; Song, B.; Peltzman, R.; Sims, D. M.; Lin, Q.; Wang, Q. Synthesis and Development of Poly(N-Hydroxyethyl Acrylamide)-Ran-3-Acrylamidophenylboronic Acid Polymer Fluid for Potential Application in Affinity Sensing of Glucose. *J. Diabetes Sci. Technol.* **2011**, *5*, 1060–1067.

(36) Okudan, A.; Altay, A. Investigation of the Effects of Different Hydrophilic and Hydrophobic Comonomers on the Volume Phase Transition Temperatures and Thermal Properties of N-Isopropylacrylamide-Based Hydrogels. *Int. J. Polym. Sci.* **2019**, *2019*, 7324181.

**JACS Au**  
AN OPEN ACCESS JOURNAL OF THE AMERICAN CHEMICAL SOCIETY

Editor-in-Chief  
**Prof. Christopher W. Jones**  
Georgia Institute of Technology, USA

**Open for Submissions**

pubs.acs.org/jacsau ACS Publications  
Most Trusted. Most Cited. Most Read.